CLOSE PROXIMITY OPERATIONS FOR A 3 NANOSATELLITES FORMATION IN LEO

Michel Delpech[(1)], Irene Valenzuela[(2)]
Centre National d'Etudes Spatiales (CNES), Toulouse, France, (33)61274775
[(1)] *michel.delpech@cnes.fr*
[(2)] *Irene.ValenzuelaMolina@cnes.fr*

ABSTRACT

In recent years, CNES has conducted several mission concept studies requiring the deployment of multiple satellites to constitute large-scale radio interferometers. ULID (Unconnected L-band Interferometer Demonstrator) is the most recent concept that involves three nanosatellites flying in close formation and that was proposed in 2017 to demonstrate the monitoring of moisture and ocean salinity with unprecedented accuracy and thus prepare the future enhancement of the SMOS program capabilities. The distributed instrument to be flown on a 600 km 6h/18h quasi-synchronous orbit requires to maintain a quasi-constant 40 meters distance between any pair of satellites using GNSS data for relative navigation and a single electric thruster for position control. Mission design studies and preliminary GNC analyses were conclusive enough to allow the transition into phase A. Unfortunately, budget restrictions in 2020 led to the project interruption at the end of phase A and the work momentum on the GNC aspects got temporarily stalled. Interestingly, ULID is expected to be reactivated in the next few years with de-scoped objectives through a low cost demonstrator that would focus on the formation flying technologies to be matured for the future deployment of radio interferometers. The first section presents the ULID formation concept and details the specific control challenges. Two control strategy options are discussed in the second section and the control design is presented. In the next section, the control performances that can be achieved for the station-keeping phase are presented for the two control strategy options and compared.

1. FORMATION CONCEPT AND CONSTRAINTS

This section presents the challenges of maintaining the formation during the interferometer measurements and the main design choices.

1.1. Formation geometry

To reach the expected resolution of the L-band interferometer [1], the optimal instrument configuration is obtained when the positions of the 3 satellites projected on the TN plane (plane perpendicular to the radial axis) form a perfect equilateral triangle that rotates at the orbital period. Such a configuration is achievable by special settings of the relative orbital elements that are presented in [2].

Another convenient representation can be based on the evolution of the relative Cartesian coordinates. The relative motion of the three satellites expressed in the orbital reference frame of the formation (center of the ellipse) can be expressed by the following equations where the coordinates x, y and z correspond respectively to the displacement in the tangential, normal and radial axis.

$$x_k(t) = A.\cos(nt + \varphi_k) \quad (1)$$
$$y_k(t) = A.\sin(nt + \varphi_k) \quad (2)$$
$$z_k(t) = A/2.\cos(nt + \varphi_k + \Delta\varphi) \quad (3)$$

with φ_k = 2(k-1).π/3 as generic setting for the different phases.

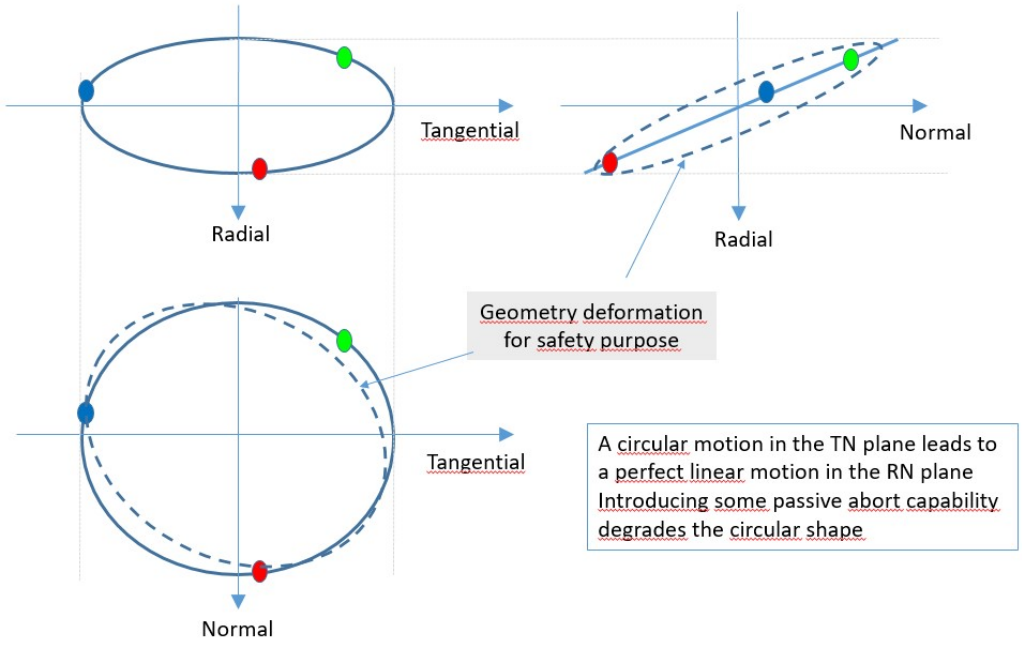

Figure 1: Formation geometry

Remark1: The phase shift $\Delta\varphi$ between the motion in the tangential-radial (TR) plane and the normal axis is supposed to be zero to ensure a perfect circular motion in the tangential-normal (TN) plane. Unfortunately, this configuration does not guarantee the absence of collisions in case any satellite starts drifting under the effect of the differential perturbations and a trade-off has to be found between the safe distance at nodal crossings and the deformation of the interferometer geometry. The phase shift is introduced for that purpose and is discussed in the next section.

In addition, the absolute localization of the formation with respect to the reference orbit can be characterized by the first satellite node argument of latitude (defined as the crossing of the TN plane with a negative velocity). This parameter will be used extensively in the rest of the document.

Passive safety

As mentioned here-above, the ULID formation geometry is not compatible with passive safety. It is well established that the inclination and eccentricity vectors constitute a good representation of the passive safety of two satellites flying in close formation [1]. Safety is maximized when the vectors are parallel (the separation is maximal when one satellite crosses the orbital plane of its companion) whereas the collision risk reaches its climax when they are orthogonal. For a formation of N satellites, the number of relative configurations amounts to $N(N-1)/2$ and this imposes to analyze the phasing of the same number of inclination and eccentricity vectors pairs.

In presence of 3 satellites some reduction of the collision risk can be obtained by modifying in the first place the phase angle between the inclination and eccentricity vectors of two satellites (for instance #2 and #3) with respect to satellite #1. The relative separation between satellites #2 and #3 is automatically imposed and must also satisfy the requirements. Fortunately, a single phase shift $\Delta\varphi$ allows to create a separation with respect to satellite #1 but allows also to ensure also a separation of the same magnitude between satellite #2 and #3. As for the magnitude of phase shift $\Delta\varphi$, it is driven by the minimum acceptable distance d_{min} according to the following expression:

$$\Delta\varphi \geq \text{asin}(d_{min}/A) \qquad (4)$$

The relative trajectories of the 3 satellites in the NR (normal-radial) plane are illustrated on Figure 2 for a 10° phase shift that corresponds to a 4 m minimum separation. It can be observed that a single phase shift allows to produce a similar deformation of the relative trajectories. This deformation can be characterized by some indexes that are associated for convenience to the inter-satellite distances. Each deformation index is defined as the distance variation divided by the reference distance. The evolution of these indexes over a single orbit is presented on Figure 2.2 for the same phase shift. It can be observed that the deformation index remains below 5% which is considered as perfectly negligible for an instrumental point of view.

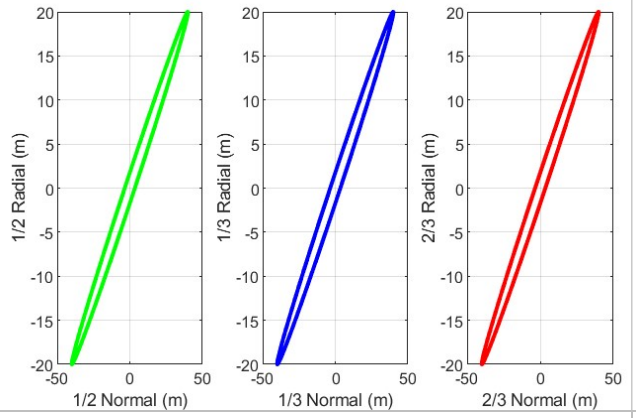

Figure 2.1: Relative trajectories of the 3 satellites in the Normal – Radial plane

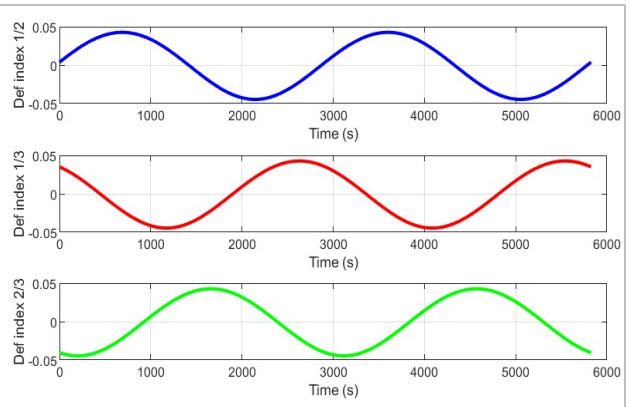

Figure 2.2: Evolution of the deformation indexes over one orbit

1.2. Satellite configuration

Each satellite is a 16U CubeSat that carries the following equipment for attitude and formation control: a SST, a GNSS receiver and a single electric thruster with a magnitude of 0.35 Nm. It carries also an ISL equipment to exchange data with its companions. The satellite mass is about 20 kg and the thruster magnitude is 0.35 Nm. The satellite layout and reference frame are presented on Figure 3. In the nominal attitude configuration (station-keeping), the solar panels are parallel to the orbital plane and the face Z+ is Nadir pointed. The thruster is accommodated on the face Y+ which allows to exert normal forces without changing the satellite attitude.

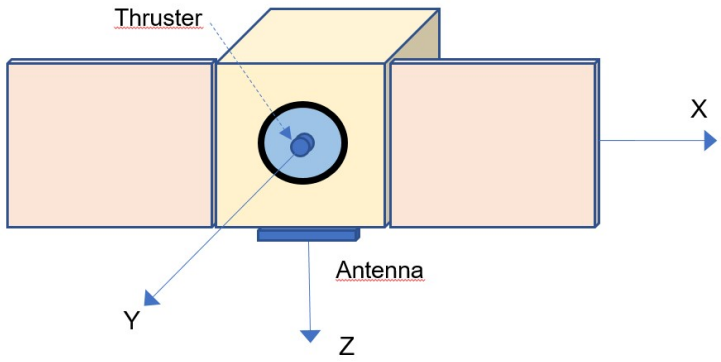

Figure 3: Satellite layout

1.3. Control constraints

The main constraints applicable to the control system are threefold and are presented here-after.

Deformation of the formation geometry:

Since the 3 satellites have different inclinations, a differential drift is produced by the J2 gravity term that affects the rate of variation of the argument of perigee $\dot{p}$ and the longitude of the ascending node g according to the following formulas:

$$\dot{p} = -(\frac{15}{2}).J_2 n.R^2(a.(1-e^2))^{-2}\sin(i).\cos(i).\delta i \quad (5)$$

$$\dot{g} = (\frac{3}{2}).J_2 n.R^2(a.(1-e^2))^{-2}\sin(i).\delta i \quad (6)$$

Note that the absolute drifts for the longitude of the ascending node and the argument of perigee are respectively 1.0 deg/day and -3.25 deg/day for a 98° inclination orbit.

In absence of control, the evolution of each satellite relative motion with respect to the anchor point can be characterized as follows:

- *Along-track deviation*: the differential drift affecting the argument of perigee cause some relative motion along the tangential axis (the relative orbit is drifting away in the TR plane)
- *Cross-track deviation*: the differential drift affecting the longitude of the ascending node is causing a phase shift of the inclination vector that introduces a distance change along the normal axis when crossing the TN plane

These deviations are different for the 3 satellites and they depend also on the formation localization that is defined by first satellite node argument of latitude. The deviations expressed in meters per day are illustrated on Figure 4 for a range of anomalies spanning the interval [0°-360°].

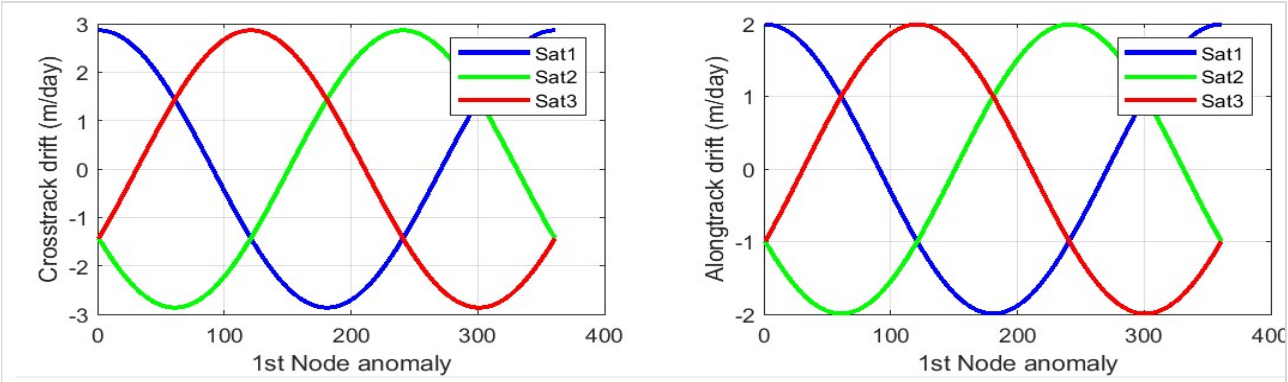

Figure 4: Evolution of the cross-track and along-track drifts depending on the formation localization

These deviations need to be compensated periodically to avoid an excessive deformation of the instrument characteristics and this implies maneuvers to be applied along the tangential and the normal axes.

Propulsion configuration:

As indicated earlier, the satellite is equipped with a single thruster that is aligned along the normal axis in normal conditions. Satellite slews are therefore required to apply maneuvers along the tangential axis or the radial axis if needed. In addition, the application of any tangential maneuver implies to turn the solar panel normal toward the velocity vector and this increases the atmospheric drag and thus the magnitude of the impulse uncertainty. This constraint is considered in more details in the sequel.

Thruster capacity:
The electric propulsion system has a low thrusting capacity. For the satellite current mass (20 kg), the thruster offers a maximum acceleration of 1.75e-5 m/s² which corresponds to 571 seconds to apply a 1 cm/s impulse (about 10% of the orbital period). In addition, the propulsion system cannot be used more than 12-19 min per orbit due to the limited power resources. This limitation represents a real constraint in the context of the formation acquisition or reconfiguration for contingency since the magnitude of the maneuvers is at least several cm/s (as an example 2.4 cm/s are needed to introduce the delta-inclinations required in the nominal configuration). Conversely, station-keeping maneuvers are in the mm/s range and can be easily executed anytime.

Thrust dispersions:
The main challenge for control comes from the thrust dispersions and particularly the direction error that creates a coupling between axes (3 sigma values for the magnitude and direction errors are respectively 15% and 5 deg). Any thrust applied along the normal axis will create a residual force along the tangential axis that is prone to produce a noticeable drift. In the worst case, a typical corrective maneuver along the normal axis with a 2 mm/s magnitude can therefore produce an impulse of 0.17 mm/s that will generate a drift of 5 m per orbit. Such a perturbation will create a fast deformation of the instrument geometry that will need to be quickly compensated.

2. CONTROL STRATEGY

2.1. Anchor point selection

Station keeping can then be performed autonomously by maintaining within specific bounds the satellite relative orbital elements that are defined with respect to some appropriate reference position (anchor point).
Different anchor point options have been proposed and analyzed:

Option A1	The anchor point corresponds to the position of a virtual satellite that evolves on a reference orbit. In this case, all satellites are rotating around this anchor point and the control is perfectly identical. The relative orbital parameters of the three satellites are precisely set so that their positions in the TN plane constantly remain on the vertices of a rotating equilateral triangle which side length is 40 m. Consequently, the satellite relative inclinations w.r.t. the “anchor” orbit must produce normal deviations with a magnitude of 40/sqrt(3) = 23.1 m.
Option A2	The anchor point corresponds to the position of one specific satellite that can be regarded as the formation master. In that case, the orbital parameters of the two companions are set w.r.t. the master ones so that their 3 positions in the TN plane form the same triangular structure that is now rotating around a vertex. Consequently, the satellite relative inclinations w.r.t. the “anchor” orbit must produce normal deviations with a magnitude of 40 m.

Note: The relative drift of the eccentricity vector phase is negligible and its adjustment has no added value. The only side effect to be considered is the drift on the tangential axis.

These two options are illustrated on Figure 5 through the use of the eccentricity and inclination vectors.

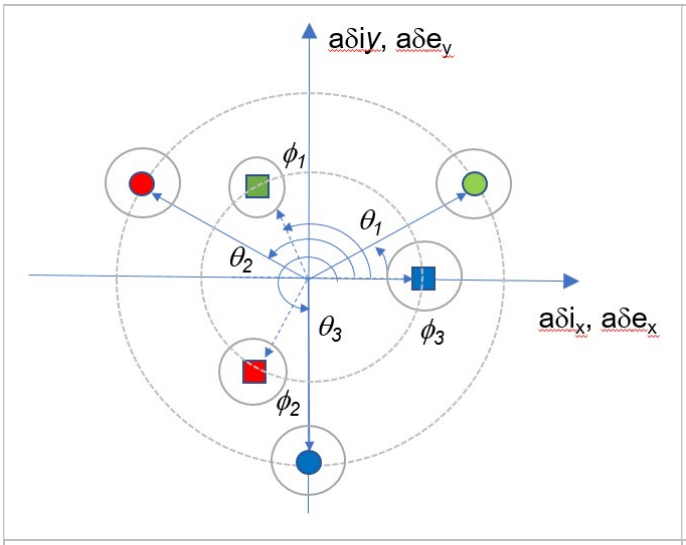

Figure 5.1: Anchor point = virtual satellite. Inclination and eccentricity vectors are represented respectively by circles and squares. The phase separation between two consecutive satellites is 120 deg

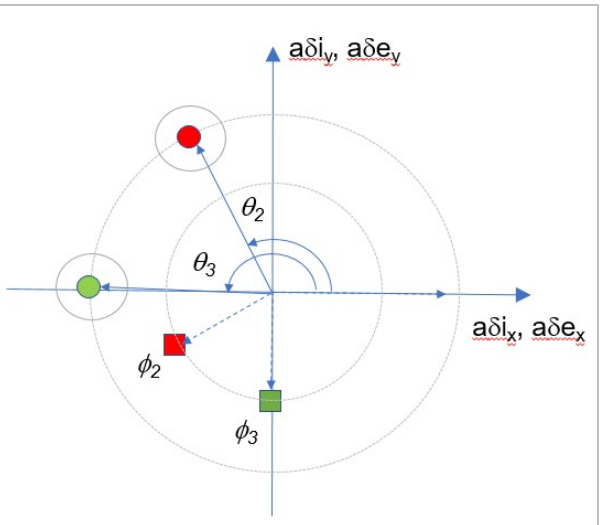

Figure 5.2: Anchor point = real satellite. The phase separation between the two active satellites is now 60 deg. Note the norm of the inclination vectors is twice larger the norm of the eccentricity vectors for both configurations

It must be outlined that the phases of the inclination and eccentricity vectors are defined as follows:

- inclination vector phase θ: argument of latitude of the formation reference object when the satellite is crossing the TR plane with a positive velocity
- eccentricity vector phase ϕ: argument of latitude of the formation reference object when the satellite reaches the largest radial deviation after the node crossing (+πi/2)

The comparison between the two options is based on several criteria that are described hereafter.

Control performance	The two options differ by the type of navigation data that is used for the formation control. If the formation anchor point is a virtual position following a reference orbit, control is based on the absolute GPS position data whereas the option 2 control relies on differential GPS data. The accuracy of differential GPS can be two orders of magnitude better than absolute GPS since the biases can be cancelled out: a few centimeters accuracy can be reached for the first one whereas the accuracy of the latter one is in the meter range [2].	
Control budget	The Option 1 configuration offers a clear benefit: the difference in their relative inclinations is smaller (ratio = 1/sqrt(3) and the relative drifts are consequently smaller. The number of maneuvers per day can be reduced along with the total budget. Conversely, Option 2 requires the control of only two satellites which offsets a large part of the control budget benefit for a single satellite. The option 1 remains more efficient than Option 2: the ratio is sqrt(3)/2 = 0.86 that corresponds only to a 14% reduction. Another aspect not taken into account in this short comparison is the budget needed in option 1 to compensate the additional tangential drift that appears between the 3 satellites of the	

	formation and the reference orbit due to the model imperfections of the atmospheric density.	

Conclusion: The second option is privileged for its better control performance and a more suitable control architecture in case of anomaly. The rest of the document will focus on this option but a comparison of the performances will be presented in the simulation results section.

Centralized versus distributed control approach

To keep the desired formation geometry in the TN plane (quasi equilateral triangle), the requirements can be expressed using the characteristics of the satellites inclination and eccentricity vectors:

- the phase difference between the inclination and the eccentricity vectors of each satellite must be constant
- the phase difference between the eccentricity vectors of the different satellites must be constant

The first requirement is obviously compatible with a distributed control approach but the question arises for the second one. Should one satellite control the phase of its eccentricity vector with respect to the other one?

The issue can be easily settled by noticing that the phase difference between the eccentricity vectors of the two active satellites has two direct causes:

- the main one corresponds to the observable differential tangential drift with respect to the anchor object
- the secondary one is the variation of the eccentricity magnitude of one active satellite with respect to the next

Controlling the mean relative position of each satellite with respect to the anchor object that serves as a common reference allows to maintain the eccentricity vector difference within bounds and this is therefore compatible with a decentralized structure.

2.2. Maneuvering approach options

To mitigate the effect of the major orbital perturbations that degrade the shape of the instrument, it is necessary to intervene in priority on the following parameters for each controlled satellite:

- correction of the relative phase and magnitude of the inclination vector
- correction of the mean tangential position offset

In addition, the magnitude eccentricity needs to be also adapted in the long run to cancel the cumulative effect of the propulsion errors induced along the radial axis.

The options to perform these different corrections are presented and discussed in the sequel.

Inclination vector control

This correction is conveniently achieved using a single maneuver along the normal axis which magnitude and phase must satisfy the following conditions [3]:

$$\delta v_n = n\left\|a\delta i - a\delta i^{ref}\right\| \quad (7)$$

$$u_M = tan^{-1}(a\delta i_y - a\delta i_y^{ref} / a\delta i_x - a\delta i_x^{ref}) \quad (8)$$

This approach is selected as baseline for ULID formation control and is illustrated on Figure 6.1.

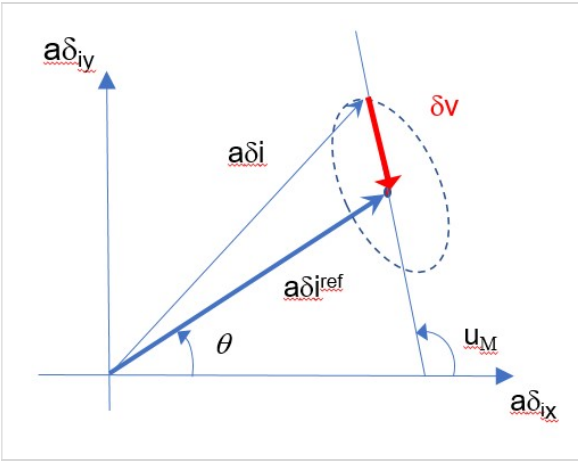

Figure 6.1 : Inclination vector correction

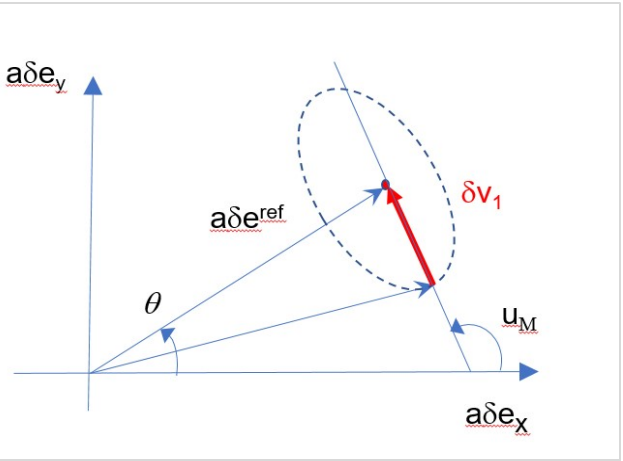

Figure 6.2 : Eccentricity vector and semi-major axis correction

Tangential drift / Mean tangential position offset and eccentricity control

Several options are considered for the control of the mean relative position and the eccentricity. They are presented on Table 1

Table 1

Option A	Combined control of tangential drift and eccentricity magnitude A classical approach to perform these corrections in a combined manner consists in using a pair of maneuvers applied along the tangential axis which magnitude and phase satisfy the following conditions: $\delta v_1 = \frac{n}{4}\left[\delta a + \left\|a\delta e - a\delta e^{ref}\right\|\right]$ (9) $\delta v_2 = \frac{n}{4}\left[\delta a - \left\|a\delta e - a\delta e^{ref}\right\|\right]$ (10) $u_{M_1} = tan^{-1}(a\delta e_y - a\delta e_y^{ref} / a\delta e_x - a\delta e_x^{ref})$ (11) $u_{M_2} = u_{M_1} + \pi$ (12) This pair of maneuvers can be used to modify the eccentricity vector without changing the semi-major axis by setting δa to 0 in the expressions (9) and (10). Conversely, this pair of maneuvers allows to slightly modify the semi-major axis to introduce a relative drift and bring back the mean relative satellite position within the acceptable bounds. The maneuver is illustrated here-above on Figure 6.2
Option B	Combined control of mean tangential position offset and eccentricity An alternate approach to correct the mean tangential position offset consists in using a pair of maneuvers applied along the radial axis. A shift of the mean relative position along the tangential axis δx is achievable with two identical impulses δv_r applied at the nodes of the relative orbit: the first impulse modifies the magnitude and the phase of the eccentricity vector whereas the second impulse rectifies the eccentricity vector properties. The introduced position shift induced by the transition phase is related to the impulse magnitude as follows: $\delta x = 2.\delta v_r / n$ (15) The total budget of the tangential position shift is therefore:

	$$\Delta v = n.\delta x \quad (16)$$ This approach has one benefit: it allows to modify the tangential position without steering the satellite to thrust along the tangential axis. However, it does not provide the capability to adapt the position drift velocity which is fundamental to ensure the control stability. This potential alternative is therefore disregarded. Note that maneuvers in the radial direction are nevertheless required to correct the magnitude of the eccentricity (see Table 2 in section).
Option C	<u>Control of tangential drift and eccentricity with maneuvers on separate axes</u> Correction of the relative tangential drift is performed with a single maneuver that can be applied anytime. This maneuver affects the semi-major axis and the relative drift according to the following expressions: $$\delta a = 2\delta v_t / n \quad (13)$$ $$\Delta v = 3\delta v_t \quad (14)$$ This single maneuver has obviously an impact on the eccentricity vector but its impact is negligible with respect to the others perturbations. The eccentricity can be nevertheless adapted if the deviation exceeds the tolerances and the control relies then on a pair of radial maneuvers applied at two successive relative node crossings. This approach has some impact on the mean tangential position offset but it is only temporary: it is suppressed after the second maneuver.

The option privileged for ULID is an adaptation of option C that is designed to mitigate the impact of the differential atmospheric drag induced during the tangential maneuvers. It is presented in the next section.

2.3. Maneuver approach with drag minimization tangential control

As indicated earlier, the application of a tangential maneuver requires to align the thruster direction with the tangential axis and this creates an increase of the atmospheric drag. In order to reduce the drag perturbing effect while mitigating the impact of the propulsion errors, it is proposed to tilt the thruster direction toward the tangential axis by a certain angle θ while keeping it in the TN plane as illustrated on Figure 7.1.

This thrusting configuration produces some velocity increment along the normal axis that can be considered as a benefit since a periodic correction is required to compensate the J2 effect. Its contribution remains however limited since the magnitude of this type of correction keeps a low value in nominal conditions. The main benefit resides in the reduction of the drag through the reduction of the satellite apparent surface and the duration of the satellite slew maneuver.

The expression of the total velocity impulse due to the atmospheric drag δv_{drag} during the whole maneuver is provided hereafter assuming an attitude slew at constant angular velocity:

$$\delta v_{drag} = \frac{1}{2}.\rho V^2.C_d.\frac{\Delta S}{m}.\left((1-cos\theta).\frac{2}{\omega_r} + sin\theta.\frac{\delta v_{com}}{a_{max}}\right) \quad (17)$$

with:

ω_r: satellite angular velocity (1 deg/s)

a_{max}: maximum satellite acceleration (1.75 e-5 m/s²)

δv_{com}: magnitude of the maneuver (variable)

ΔS: additional satellite surface for θ = π/2 (0.25 m²)

m: satellite mass (20 kg)

ρ: atmospheric density (variable)

C_d: satellite drag coefficient (2.2)

The satellite configuration during thrust and the attitude profile during the whole maneuver including slew are respectively illustrated on Figure 7.1 and Figure 7.2

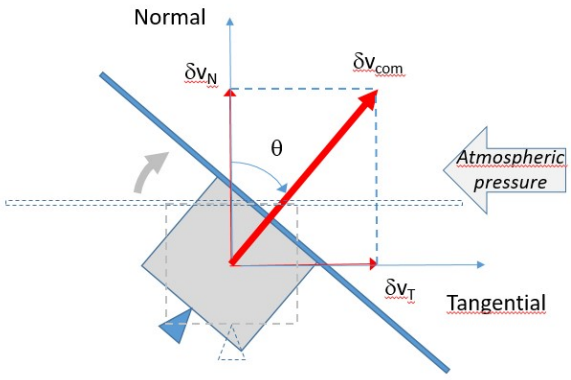

Figure 7.1: Satellite in thrust configuration

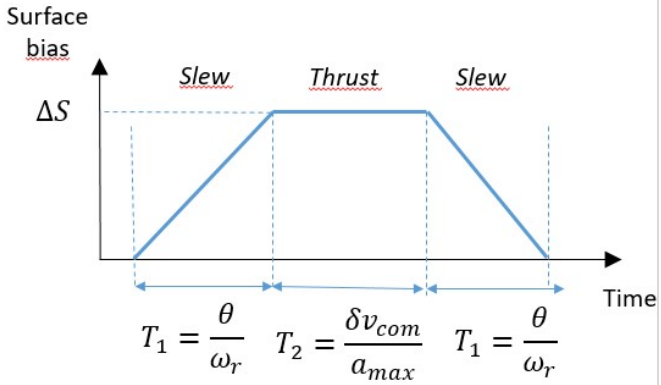

Figure 7.2: Satellite attitude profile during the maneuver

The velocity impulse due to the atmospheric drag is a perturbation that is added to the commanded tangential impulse or subtracted from it depending on its direction. It is therefore paramount to determine the envelope of conditions within which the perturbation magnitude remains sufficient lower than the commanded impulse. The parameters to be considered include the atmospheric density ρ, the satellite inclination angle θ and the maneuver magnitude δv_T. A preliminary analysis will tend to privilege small inclinations angles that enable to reduce both the satellite dragging surface and the duration of the slew maneuver. Conversely, the relative impact of the propulsion direction error is increasing for low inclinations and will offset at some point the benefit of a reduced drag perturbation. The full analysis consists in finding the maneuver inclination that is properly addressing the propulsion – drag perturbation tradeoff. The notion of perturbation ratio is introduced for that purpose and corresponds to the magnitude of the perturbation impulse divided by the magnitude of the commanded tangential impulse. The drag perturbation ratio is computed for different inclination angles from 1° to 40° and for a range of atmospheric densities that can be encountered on a 700 km quasi circular orbit [$2e^{-13}$ – $2e^{-12}$ kg/m^3]. The propulsion perturbation ratio is only dependent on the inclination angle and is computed for the same range [1° - 40°]. The computation is based on the following propulsion errors [3% magnitude (1σ), 1.5° direction (1σ)]. The tradeoff results are produced for two different maneuver magnitudes that are translated into the associated relative position drift expressed in meters per orbit. The two reference values are 1 m/orbit and 3 m/orbit that correspond respectively to a low and high commanded drifts (see Figures 8.1 and 8.2). It can be observed that the best inclination angle is close to 10° for the highest atmospheric density but can be increased for lower density values and for larger drift amplitudes. In addition, the perturbation ratio can be brought down to 15% in the worst case (drift = 1 m/orbit).

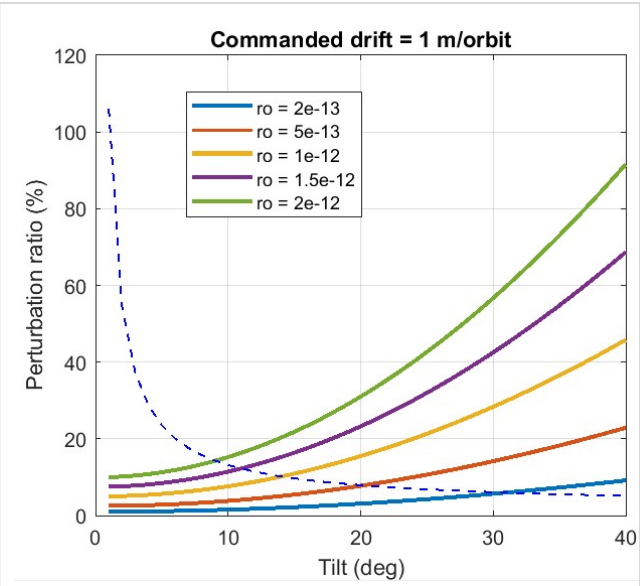

Figure 8.1 : Evolution of the perturbation ratio evolution when commanding a low tangential drift

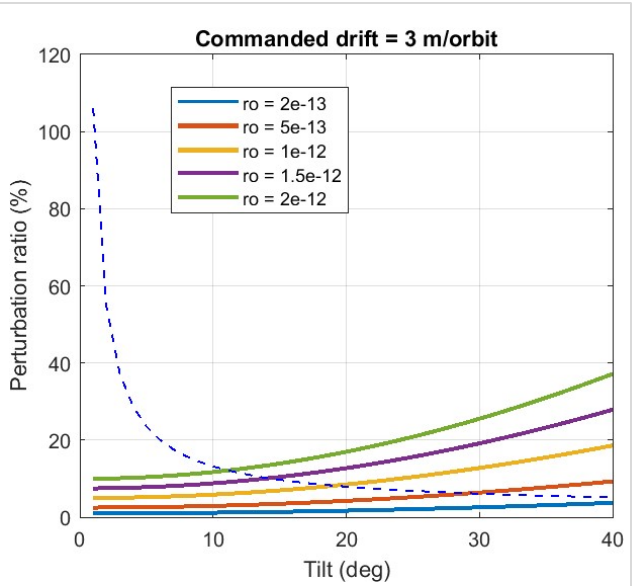

Figure 8.2 : Evolution of the perturbation ratio evolution when commanding a high tangential drift

The tangential drift corrective maneuver is computed according to the following algorithm:

- The maneuver is scheduled when the position bias or the drift rate exceed specific thresholds (typical values for the boundary box are +/- 5 meters)
- The date of maneuver is set such that the phase of the normal motion is π/2 or 3π /2 depending on the current phase: the selected phase is the closest achievable taking into account the time required for the attitude slew maneuver. Selecting a phase where inclination maneuvers are usually executed allows to not impact the phase of the inclination vector.
- The expression of the maneuver magnitude that depends on the drift rate and the current position offset is given here-after:

$$\delta v_T = (d_{est} + d_{bias})/(3.T) \qquad (18)$$

with

d_{est} : estimated tangential drift expressed in meters per orbit,

d_{bias}: bias drift within the bounds of the tangential control box expressed in meters per orbit

T: orbital period

Note: the value of the bias drift is null when the maneuver is scheduled for a drift rate overflow. In case of position boundary overflow, a drift bias value of 0.5 m/orbit ensures a slow

Following the above mentioned analysis, the adopted control approach is based on 3 types of maneuvers which main characteristics are summarized in Table 2

Table 2

Inclination control	- Single maneuver along the normal axis - The maneuver is scheduled when the angle difference between the current and desired phase of the inclination vector exceeds a given threshold - The magnitude and dates are set according to formula (7) and (8) – the date of application corresponds to a phase of π/2 or 3π/2 for the normal motion

	- The typical magnitude is in the 2-3 mm/s range for an activation every 6-7 orbits
Tangential control	- Maneuvers with a slight tilt along the tangential axis (ex: 10 deg) - The maneuver is scheduled when the position bias or the drift rate exceed specific thresholds - The date corresponds to a phase of $\pi/2$ or $3\pi/2$ for the normal motion and the magnitude is set according to formula (18) - The maneuver frequency is directly correlated with the magnitude of the thrust direction error
Eccentricity control	- Single maneuver along the radial axis - The maneuver is scheduled when the norm of the eccentricity vector exceed some tolerances $[y_m - \delta y_{max}, y_m + \delta y_{max}]$ - The date corresponds to a phase of 0 or π for the motion in the TR plane - the selected phase is the closest achievable taking into account the time required for the attitude slew maneuver - The maneuver frequency is low since the deviation is only due to the cumulative effect of the thrust direction errors

2.4. Relative state estimation

For each active satellite, the relative control is relying on the following data provided by the GPS system

- Formation argument of latitude: this measurement should concern the formation anchor object but the measurement given by the current GPS receiver is definitely accurate enough
- Relative Position / Velocity / Time vector with respect to the formation anchor object: this measurement is obtained through the processing of differential GPS data

The relative Position / Velocity vector has a good intrinsic accuracy but the ability to estimate precisely the mean motion characteristics at any time is made difficult by the amplitude of the oscillations along the 3 axes. This statement is particularly true for the tangential drift that is most challenging to determine.

The mean motion characteristics are therefore estimated at some specific epochs (nodes crossings) using only the relative position information:

- *Cross-track deviation*: this deviation is updated at every single crossing of the reference TN plane (both ascending and descending phases)
- *Along-track deviation*: this deviation is computed from two different offset variables X_{plus} and X_{minus} that are updated when the satellite is crossing the reference TN plane with respectively a positive velocity and a negative velocity.

$$\delta X_{est} = \left(X_{plus} + X_{minus}\right)/2 \qquad (19)$$

- An estimation of the drift rate d_{est}expressed in meters per orbit is obtained by considering the variation of the along-track deviation that is updated at every crossing of the TN planes. The drift rate is obtained by multiplying this variation by 2 since the update intervenes twice per orbit.

$$d_{est} = 2(\delta X_{est}(k) - \delta X_{est}(k-1)) \qquad (20)$$

2.5. Passive safety evolution

As indicated in section 1, a small phase shift must be introduced to create a cross-track separation when the satellite is crossing the RN plane. However, the phase shifts of the different satellites do not remain constant due to the J2 effect and the evolution of their magnitude needs to be taken into account to ensure passive safety over a given time horizon. This evolution is also dependent on the latitude of the formation first node as illustrated on Figures 9.1 and 9.2 that present the variation of the cross-track drift for the 2 options (3 satellites and 2 satellites).

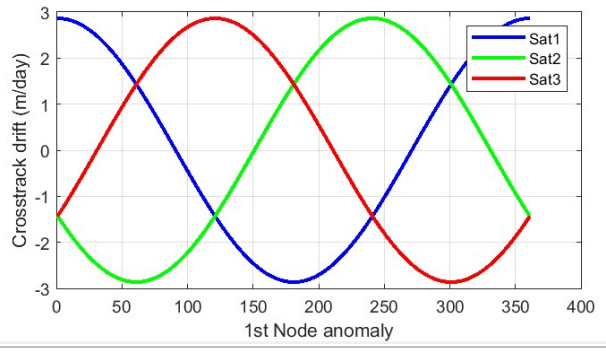

Figure 9.1: Option 1 (3 active satellites)

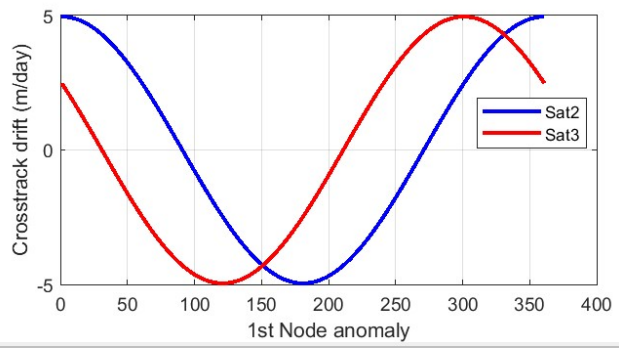

Figure 9.1: Option 2 (2 active satellites)

The cross-track drift can be positive or negative depending on the latitude of the formation first node. A positive drift will increase the separation and reduce the collision risk. Conversely, a negative drift will reduce the separation unless the sign of the phase shift is also negative. To ensure that the collision risk margin is not decreasing over time in all circumstances, some strategy must be implemented for each active satellite:

- the sign of the phase shift is selected depending on the latitude of the formation first node (positive if the drift is positive, negative otherwise)
- the sign of the phase shift is modified when the sign of the cross-track drift changes - the effective modification intervenes at the next inclination correction opportunity (when the phase difference exceeds a fixed threshold) – this phase shift is to be done roughly every 60 days (that corresponds to a 180° phase shift of the eccentricity vector).

Remark: This approach is perfectly applicable to both options and the configuration changes are nominally performed by the ground.

Formation reconfiguration

Selecting one of the satellites as the formation anchor object imposes periodic reconfigurations to balance the propellant budget. The transition steps are the following:

- control switch-off of the satellite designated as the new anchor object
- configuration change of the GPS Navigation system for the two active satellites: the relative state is computed with respect to a new satellite reference
- control initialization and switch-on of the satellite that was previously inactive (previous anchor object) - the initialization step consists in setting the phase angle of the eccentricity vector

Note: The reconfiguration is nominally performed by the ground.

2.6. GNC Architecture

This GNC architecture for all satellites and its main components illustrated on Figures 10.1 and 10.2.

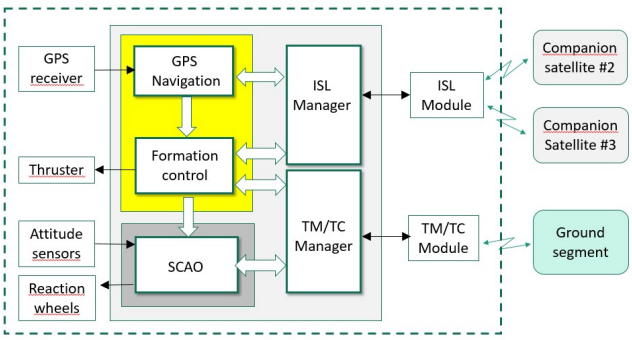

Figure 10.1: Overall GNC architecture

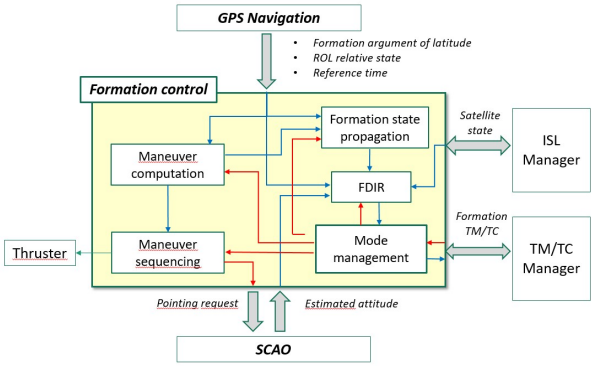

Figure 10.2: Components of the formation control module

Each satellite is interacting with its two companions via an inter satellite link to exchange state data and GPS raw dat. It includes a GPS Navigation module that processes the measurements from its own GPS receiver and combines them with the equivalent data provided by the companion satellites. This module is designed to estimate the relative state of each satellite of the formation with high accuracy (position at centimeter level) and provides also the absolute localization of the current satellite.

The formation control module is mainly responsible for the orbital maneuver computation but the maneuver execution is also considered. For that purpose, this module is interfaced with the attitude control system to request attitude slew maneuvers. Maneuvers are computed and scheduled according to the overall control approach described in section 2.5. The module integrates also a FDIR subsystem that deals with the different contingency cases and triggers if necessary some reconfiguration or anti-collision maneuvers [2].

3. CONTROL APPROACH AND PERFORMANCE ANALYSIS

This section presents the control performances that can be achieved in station keeping for option 2 and performs a first analysis of their variability. Next, it presents the control behavior during the nominal reconfiguration (switch between anchor points) that has to be performed periodically in this control strategy. Next, some simulations are run with Option 1 to perform a preliminary comparison between the two options.

3.1. Station-keeping (Option 2)

The control behavior is analyzed using a simulator of the formation that relies on a simplified gravity model including only the central and J2 terms. Atmospheric drag effects are considered as differential perturbations that intervene when the satellite attitude is driven away from the nominal configuration. Thrust perturbations are introduced on each maneuver according to the error model mentioned in section 1.3. Finally, GPS navigation errors are also introduced with the following 1 sigma magnitude: 5 cm (position) – 0.1 mm/s (velocity).

The nominal scenario used for the illustration is initialized as follows: Satellite #1 is the anchor object and its argument of latitude is null. Satellites #2 and #3 are set on their desired relative orbits with an initial phase of 0 and $\pi/6$ respectively. No passive safety is being introduced ($\Delta\varphi = 0$) to better illustrate the control performance using the deformation index. The satellites are also affected by some initial tangential drift (0.01 mm/s). Control parameters are the following: the tangential position tolerance is +/-5m, the inclination maximum phase shift is 4 degrees and the maximum relative error of both inclination and eccentricity vectors magnitude is 5 %. The atmospheric density considered for the simulation is set at a high value ($1e^{12}$ kg/m^3) to evaluate the benefit of the drag minimization approach.

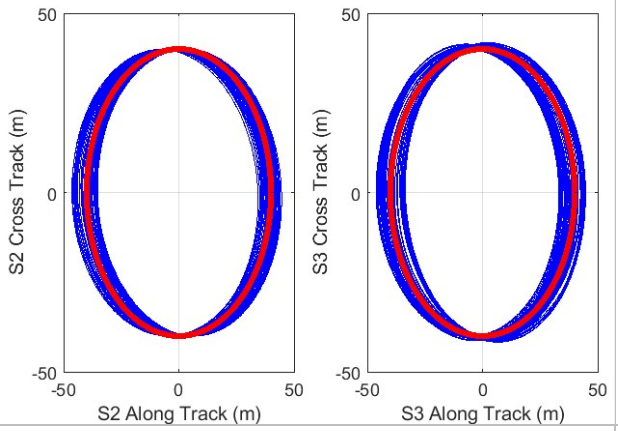

Figure 11.1: Relative motion of satellites 2 and 3 with respect to the anchor object

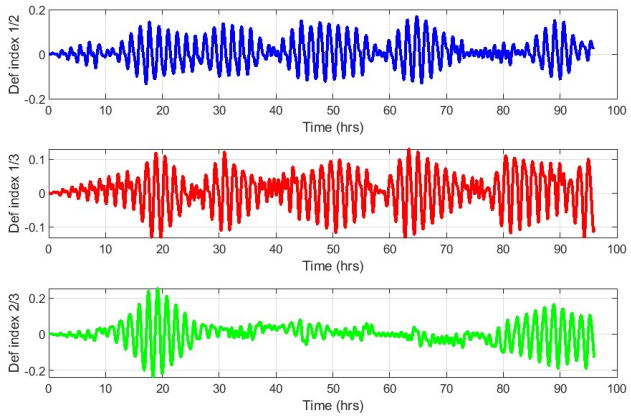

Figure 11.1: Deformation indexes of the three inter-distances

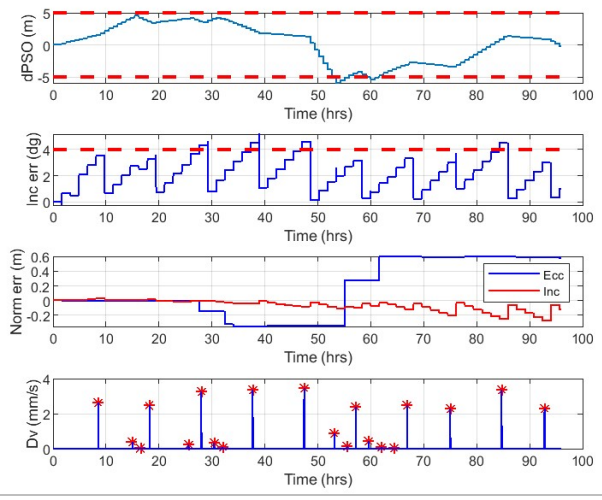

Figure 12.1: Control behavior of satellite #2

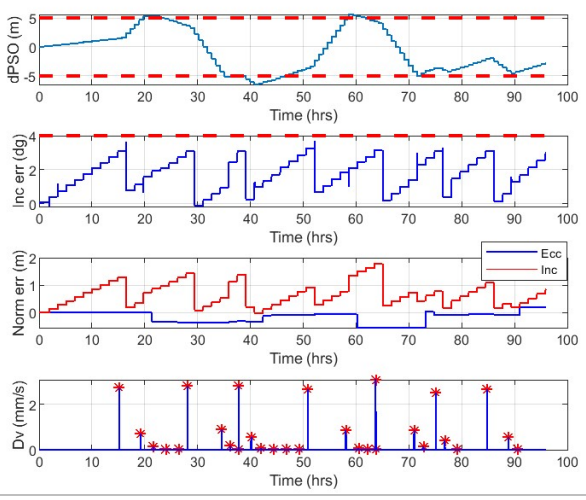

Figure 12.2: Control behavior of satellite #3

The control behavior of the two satellites is illustrated on Figures 12.1 and 12 and is characterized by the following indicators (1) the position error on the tangential axis, (2) the inclination vector phase error, (3) the errors on the norms of the eccentricity and inclination vectors, (4) the maneuvers magnitude. The total impulse for 4 days is 5.4 cm/s and is mainly based on the inclination corrective maneuvers that appear with the larger magnitude. All other maneuvers correspond to the tangential drift control since no radial maneuvers are actually applied: the eccentricity observable variations are only caused by the dispersions of the normal or quasi normal maneuvers. Regarding the deformation index, it directly represents the control performance and its value gets up to 0.15 for the distance between the active satellites and the anchor point. As a consequence, the deformation between the two active satellites (Def index 2/3) exceeds 0.2 when the errors are approximately phased. In real mission conditions where some additional separation is introduced to ensure passive safety, the maximum deformation will be in the 0.25 range that is near the targeted tolerance requirement (0.3).

The budget variability is further analyzed by performing multiple runs in two different contexts: (1) the argument of latitude of the first node is constant but the random number generator is initialized with different seeds, (2) the argument of latitude of the first node is spanning the interval [0-2π]. The number of simulation runs for this analysis is 50.

	Same initial state	Formation phase
Mean value (cm/s)	5.88	5.1
Standard deviation (cm/s)	0.65	1.24

These figures that represent the control behavior for Option 2 in nominal conditions are set as reference to allow a performance comparison with option 3.

3.2. Nominal reconfiguration (Option 2)

Simulation results that feature such a transition are presented in this section for illustration only. The initial configuration is similar to the one from the previous test (satellite #1 is the anchor point). A reconfiguration and consists in selecting satellite #2 as anchor point intervenes after 1 day.

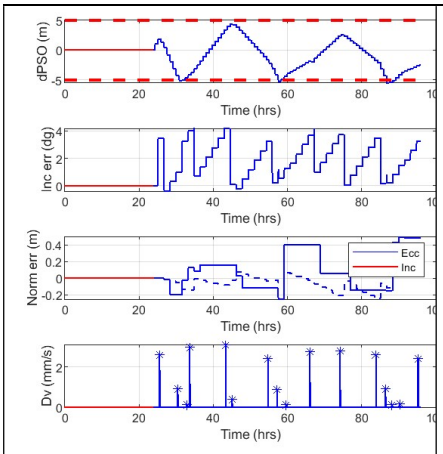

Figure 13.1: Control behavior of satellite #1

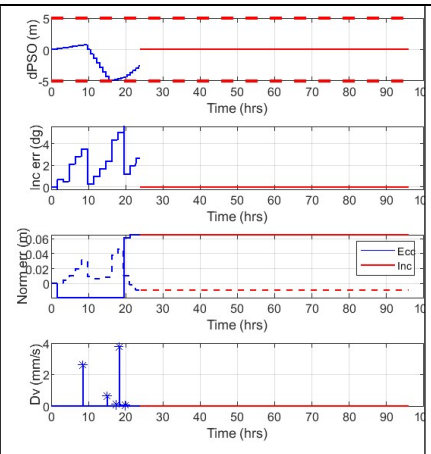

Figure 13.2: Control behavior of satellite #2

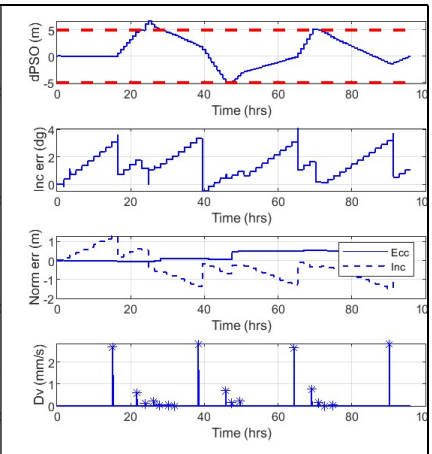

Figure 13.3: Control behavior of satellite #3 (always active)

The transition is clearly observed on Figures 13.1 and 13.2 where the parameters associated to the inactive phase are null and plotted in red. When satellite #1 is activated, the residual errors that were seen by satellite #2 are detected with equivalent amplitude after some initialization and estimation phase (the position error on the tangential axis is logically seen with an opposite sign). As for satellite #3 behavior, transitioning from a reference point to the next is barely noticeable on the error plots. This simulation shows that the control behavior is not expected to be negatively impacted by the anchor object change.

3.3. Station-keeping (Option 1)

A simplified error model has been introduced for the GPS absolute navigation data and consists in varying biases affecting the 3 position components that are represented by sinus functions with identical magnitudes but different frequencies and phases:

- the magnitude has been voluntarily set to some optimistic value (1 m)
- the frequencies on the x, y and z components are constant multiples of the orbital frequency with the following values [5.1 4.2 3.2] and the phases are [0, 2π/3, 4π/3] that ensure different biases at the nodes crossings

It must be outlined that preliminary tests with different frequencies and phases do not generate any noticeable variation of the overall behavior. Conversely, the main impact is actually due to the bias magnitude.

The nominal scenario used for a first illustration of the behavior is initialized as follows: the argument of latitude of the anchor object is null. Satellites #1, #2 and #3 are set on their desired relative orbits with initial phases of 0, 2π/3 and 4π/3 respectively. The satellites are also affected by some initial tangential drift (0.01 mm/s). As for the control parameters, they have been taken identical to the ones considered for the Option 2 configuration.

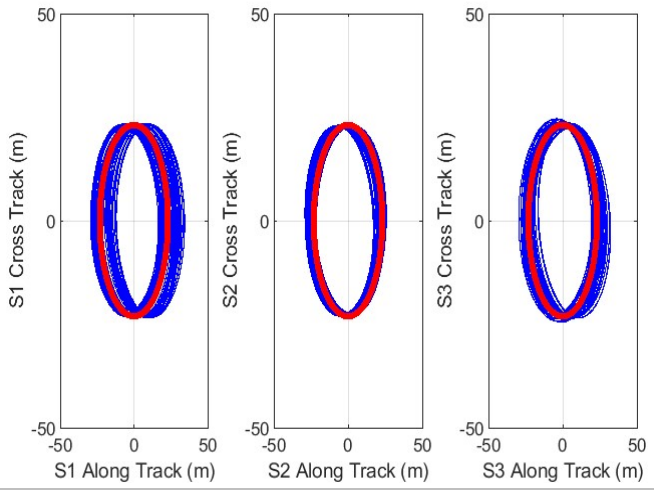

Figure 14.1: Relative motion of satellites 1, 2 and 3 with respect to the anchor object

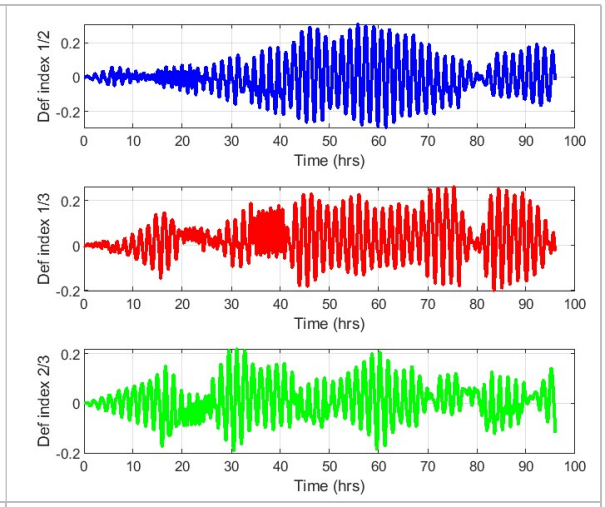

Figure 14.2: Deformation indexes of the three inter-distances

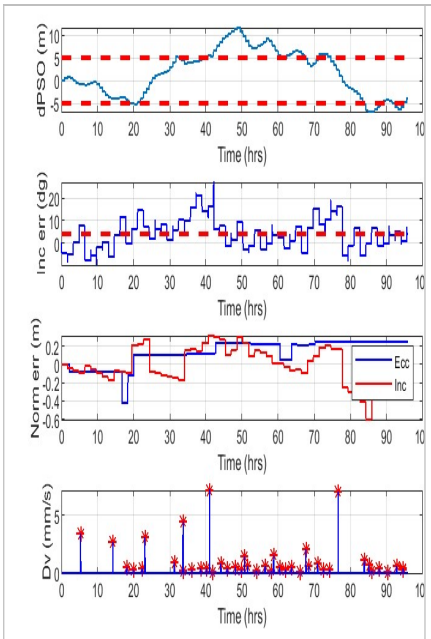

Figure 15.1: Control behavior of satellite #1

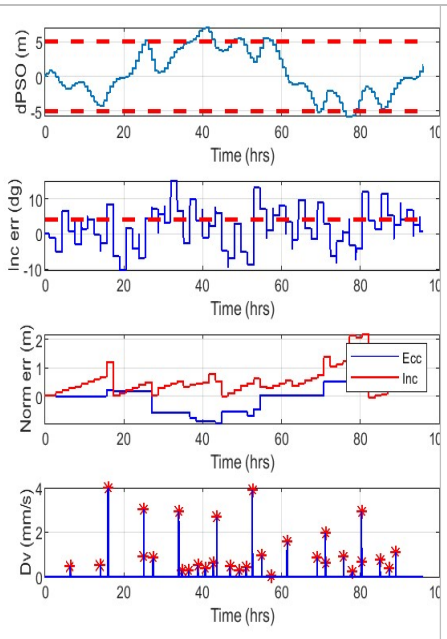

Figure 15.2: Control behavior of satellite #2

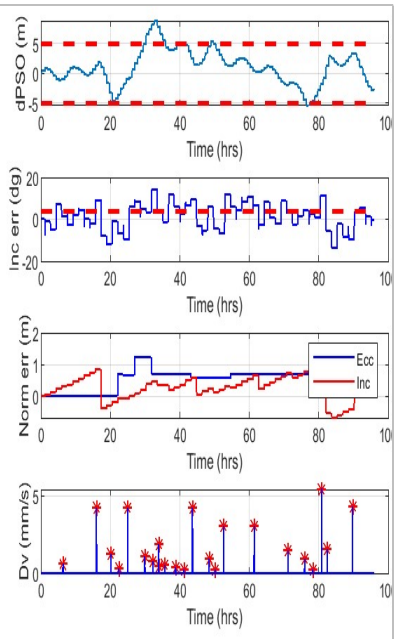

Figure 15.3: Control behavior of satellite #3

Figures 15 show a clear degradation of the control performance for both the tangential position and the phase of the inclination vector. This first impact is directly caused by some inaccurate estimation of the tangential drift that induce a large number of corrective maneuvers. These maneuvers performed with a 10° tilt and a magnitude close to 1 mm/s in many occasions affect negatively the phase of the inclination vector.

The budget variability is then analyzed with the same approach applied to option 2 and the results are presented on the following table. An increase by a factor of 2 can be observed even though the test

conditions are made rather favorable for this option: the bias magnitude is set at a level remarkably optimistic and the control bounds have not been resized proportionally to the formation geometry.

	Same initial state	Formation phase
Mean value (cm/s)	11.23	10.83
Standard deviation (cm/s)	0.97	1.08

This first evaluation needs to be completed with a more representative GPS error model and appropriate control bounds but it shows nevertheless a tendency that supports the preference for the option 2 control strategy.

4. CONCLUSION

This paper has presented the specific control challenges to be faced for the realization of the ULID distributed instrument based on three nanosatellites flying in close formation. Two different options have been analyzed for the control strategy: the formation reference point is either a virtual object following a predefined orbit or one satellite of the formation. The analysis based on navigation performance considerations has shown that the second option is the most favorable and this tendency has been confirmed through simulations. In addition, a specific maneuvering approach has been proposed to deal with the propulsion system limitations and the impact of the differential atmospheric drag. Preliminary simulation campaigns using simplified models for the GPS absolute navigation data and the differential drag produce promising results that will need some consolidation in the next phase of the project.

5. REFERENCES

[1] F. Cabot & al, A Demonstration Mission for Distributed L-band Interferometry Earth Observation, 2021 IEEE International Geoscience and Remote Sensing Conference

[2] A. Lamy & al, Close Satellite Formation Flying for ULID mission, 11th International Workshop on Satellite and Constellation Formation Flying, Milano, Italy,

[3] S. Damico & al, Relative Orbit Control Design for the PRISMA Formation Flying mission, AIAA Guidance and Navigation Control Conference, August 2006